© 2014. Published by The Company of Biologists Ltd | Development (2014) 141, 2611-2620 doi:10.1242/dev.107078

RESEARCH ARTICLE

STEM CELLS AND REGENERATION

Nuclear to cytoplasmic shuttling of ERK promotes differentiation of muscle stem/progenitor cells

Inbal Michailovici[1], Heather A. Harrington[2], Hadar Hay Azogui[1], Yfat Yahalom-Ronen[1], Alexander Plotnikov[1], Saunders Ching[3], Michael P. H. Stumpf[2], Ophir D. Klein[3,4], Rony Seger[1] and Eldad Tzahor[1,*]

ABSTRACT

The transition between the proliferation and differentiation of progenitor cells is a key step in organogenesis, and alterations in this process can lead to developmental disorders. The extracellular signal-regulated kinase 1/2 (ERK) signaling pathway is one of the most intensively studied signaling mechanisms that regulates both proliferation and differentiation. How a single molecule (e.g. ERK) can regulate two opposing cellular outcomes is still a mystery. Using both chick and mouse models, we shed light on the mechanism responsible for the switch from proliferation to differentiation of head muscle progenitors and implicate ERK subcellular localization. Manipulation of the fibroblast growth factor (FGF)-ERK signaling pathway in chick embryos *in vitro* and *in vivo* demonstrated that blockage of this pathway accelerated myogenic differentiation, whereas its activation diminished it. We next examined whether the spatial subcellular localization of ERK could act as a switch between proliferation (nuclear ERK) and differentiation (cytoplasmic ERK) of muscle progenitors. A myristoylated peptide that blocks importin 7-mediated ERK nuclear translocation induced robust myogenic differentiation of muscle progenitor/stem cells in both head and trunk. In the mouse, analysis of Sprouty mutant embryos revealed that increased ERK signaling suppressed both head and trunk myogenesis. Our findings, corroborated by mathematical modeling, suggest that ERK shuttling between the nucleus and the cytoplasm provides a switch-like transition between proliferation and differentiation of muscle progenitors.

KEY WORDS: ERK, FGF signaling, Myogenesis, Chick, Mouse

INTRODUCTION

Myogenesis, the formation of muscle tissue, takes place during embryonic development, postnatal growth and regeneration. Myogenesis begins with the commitment of mesoderm precursor cells to the myogenic lineage. This is followed by proliferation of myoblasts and their differentiation into postmitotic myocytes that fuse to form multinucleated myotubes. Previous genetic studies in mice suggest that skeletal muscles have evolved to use distinct regulatory networks upstream of the myogenic regulatory factors (MRFs) to initiate myogenesis at different anatomical locations (e.g. head and trunk) (Buckingham and Vincent, 2009).

[1]Department of Biological Regulation, Weizmann Institute of Science, Rehovot 7610001, Israel. [2]Theoretical Systems Biology, Division of Molecular Biosciences, Imperial College London, London SW7 2AZ, UK. [3]Department of Orofacial Sciences and Program in Craniofacial and Mesenchymal Biology, University of California San Francisco, San Francisco, CA 94143-0430, USA. [4]Department of Pediatrics, Institute for Human Genetics, University of California San Francisco, San Francisco, CA 94143-0442, USA.

*Author for correspondence (eldad.tzahor@weizmann.ac.il)

Received 12 December 2013; Accepted 30 April 2014

There are approximately 60 distinct skeletal muscles in the vertebrate head that control eating, facial expression and eye movement. In recent years, interest in this unique group of skeletal muscles has significantly increased, with the accumulation of lineage tracing, molecular profiling and gene targeting studies (Noden and Francis-West, 2006; Grifone and Kelly, 2007; Sambasivan et al., 2011; Tzahor and Evans, 2011). Mesoderm cells located anterior to the somites give rise to skeletal muscle precursors in the head. Pharyngeal mesoderm precursors fill the myogenic core within the pharyngeal arches (Tzahor and Evans, 2011), where cranial neural crest cells surround the muscle anlagen, separating the myoblasts from the overlying surface ectoderm (Noden, 1983; Trainor et al., 1994).

In comparison with the trunk, the molecular mechanisms underlying head myogenesis are in general less characterized. It is known that BMP and Wnt/β-catenin pathways are potent regulators of trunk and head mesoderm progenitors (Buckingham, 2006). Manipulation of these signaling molecules in chick embryos resulted in distinct myogenic responses in the head and trunk regions (Tzahor et al., 2003). In addition, BMP and FGF-ERK signaling play opposing roles in the proliferation and differentiation of anterior heart field progenitors, which are also derived from the pharyngeal mesoderm. FGF-ERK signaling blocks the premature differentiation of these heart progenitors, highlighting the importance of blocking FGF signaling as a key step in the differentiation of cardiomyocytes (Tirosh-Finkel et al., 2010).

FGF signaling affects skeletal muscle progenitors in several ways, promoting both progenitor cell proliferation and their differentiation, depending on the cellular and spatiotemporal contexts. Myoblasts grown in culture start to differentiate, when the amount of growth factors in the media is reduced. The key growth factor repressing myogenic differentiation in these cultures was found to be FGF (Olwin and Rapraeger, 1992). In the chick embryo, *Fgfr4* is expressed in $Myf5^{+}$ $MyoD^{+}$ myogenic cells in the limb (Marcelle et al., 1995); in the mouse, this gene is directly regulated by *Pax3* (Lagha et al., 2008). Forced expression of *Fgf8* in the chick somites upregulated *Fgfr4* expression and enhanced myogenic differentiation. Likewise, electroporation of a dominant-negative *Fgfr4* inhibited myogenic differentiation (Marics et al., 2002). Together, these *in vivo* studies suggest that FGF signaling is required for trunk myogenesis.

Extracellular signal-regulated kinase 1/2 (ERK, also known as p42/44 mitogen-activated protein kinase MAPK) can be activated by a variety of growth factors/mitogens (such as FGF) and it has many substrates. The majority of studies in the field have been carried out in cultured myoblasts, and these have shown that ERK is crucial for growth factor-induced cellular proliferation of myoblasts and subsequently for myoblast fusion (Jones et al., 2001; Knight and Kothary, 2011), making ERK a key regulator of both myoblast proliferation and differentiation. During proliferation, ERK activity

Development (2014) 141, 2611-2620 doi:10.1242/dev.107078

prevents cell cycle exit during G_1 (Heller et al., 2001). However, it has been shown that ERK2 is required for efficient terminal differentiation of skeletal myoblasts (Li and Johnson, 2006).

In the current study, we investigated the role of ERK signaling during muscle development both *in vitro* and *in vivo*. Pharmacological perturbations along the FGF-ERK signaling cascade or solely blockage of ERK nuclear translocation were sufficient to induce myogenic differentiation. We suggest that FGF-mediated ERK nuclear translocation represses the differentiation of embryonic muscle progenitors and adult muscle satellite cells. Our findings, corroborated by mathematical models, further suggest that the bi-directional nuclear translocation of ERK is optimally suited to act as a cell fate regulator.

RESULTS

Head muscle precursors undergo robust myogenesis in culture after 4 days, roughly at the same kinetics that occurs *in vivo* (Fig. 1A,B) in agreement with previous studies (Tzahor et al., 2003; Rinon et al., 2007; Harel et al., 2009). Explants of the pharyngeal mesoderm with its adjacent tissues, ectoderm and endoderm (termed PMEE), were cultured *ex vivo* to examine the dynamic molecular profiles of head myogenesis with a focus on FGF ligands. RT-PCR analysis of PMEE explants cultured for 1 day revealed no expression of the myogenic differentiation markers *MyoD* (*Myod1* – Mouse Genome Informatics), *Myog* and *MHC* when compared with the same explants at 4 days, when these markers are strongly upregulated (Fig. 1B). In contrast to the myogenic genes, FGF ligands were expressed at high levels on day 1 and expression was reduced with the onset of myogenic differentiation, on day 4 (Fig. 1B). qRT-PCR verification of our culture system demonstrate a reduction in cyclin D1 (*Ccnd1*) compared with upregulation of MyoD that occurred in differentiating PMEE explants (Fig. 1C).

In situ hybridization of MyoD along with members of the FGF signaling network, at stage 16 and 20 chick embryos showed that FGF signaling is negatively correlated with head myogenesis, confirming our findings in culture (Fig. 1D and supplementary material Fig. S1). The expression of known FGF target genes (*Sef*, *Erm*, *Pea3* and *Mkp3*; *Il17rd*, *Etv5*, *Etv4* and *Dusp6*, respectively – Mouse Genome Informatics) was downregulated with the onset of myogenic differentiation (stage 20), reinforcing the negative correlation between FGF signaling and head myogenesis (Fig. 1D and supplementary material Fig. S1). Immunostaining for pERK at stages 14-16 revealed strong expression in neural crest cells (marked by AP2) but later its expression was detected also within the myogenic core (Fig. 1E, circle). At stages 18-20, pERK expression was significantly reduced with the onset of differentiation. Taken together, these findings suggest that FGF signals block premature differentiation of both cardiac (Tirosh-Finkel et al., 2010) and pharyngeal muscle progenitors (Fig. 1 and supplementary material Fig. S1).

Next, we examined whether inhibition of FGF signaling is sufficient to promote head myogenesis *in vitro* and *in vivo*. Inhibition of FGF signaling using SU5402, a pharmacological inhibitor of the FGF receptor [and of other receptor tyrosine kinases (RTKs), see Discussion], promoted robust myogenesis, accompanied by reduced *Ccnd1* expression and upregulation of the cell cycle inhibitor *p21* (Fig. 2A). In contrast, infection of PMEE explants with FGF8-RCAS

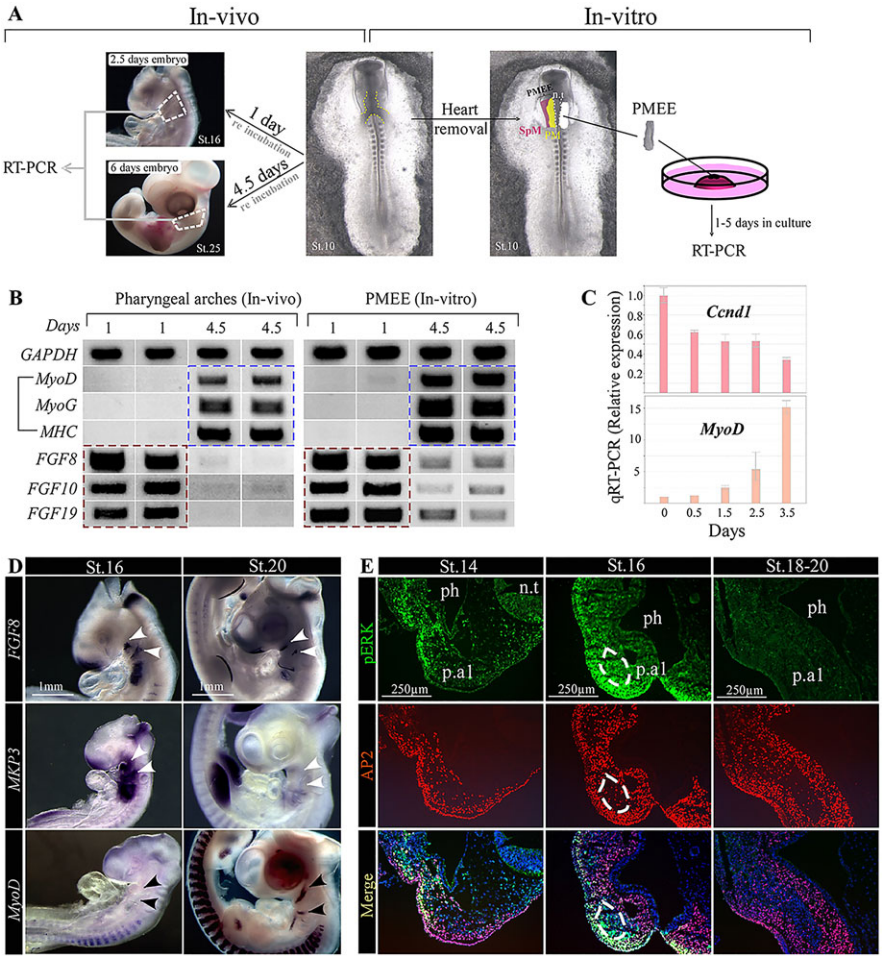

Fig. 1. FGF-ERK signaling is reduced with the onset of myogenic differentiation in the chick. (A) Schematic experimental setting of the dissection of PMEE explants and pharyngeal arches in chick embryos. PMEE explants were dissected from stage 10 chick embryo and cultured for 1 or 4.5 days. Control stage 10 embryos were grown in an incubator for 1 or 4.5 days and their pharyngeal arches were then dissected. (B) Pharyngeal arches and the PMEE explants were further analyzed by RT-PCR for skeletal muscle markers (black bracket) and for FGF ligands. The red lines indicate downregulated genes, whereas blue lines indicate genes that were upregulated during myogenesis. These results represent more than three independent experiments, each performed in duplicates composed of a pool of five explants. (C) qRT-PCR verification of the relative expression of the indicated genes. Data are mean±s.d. (D) Comparison of gene expression during chick myogenesis (from stages 16-20), using whole-mount *in situ* hybridization. White arrowheads indicate downregulated genes; black arrowheads indicate upregulated genes. (E) Immunofluorescence on transverse sections at the level of the first pharyngeal arch of stage 14-20 chick embryo, stained for DAPI, pERK and the neural crest cell marker AP2. The mesodermal core is outlined. n.t, neural tube; SpM, splanchnic mesoderm; PM, pharyngeal mesoderm; ph, pharynx; p.a1, first pharyngeal arch.

Development (2014) 141, 2611-2620 doi:10.1242/dev.107078

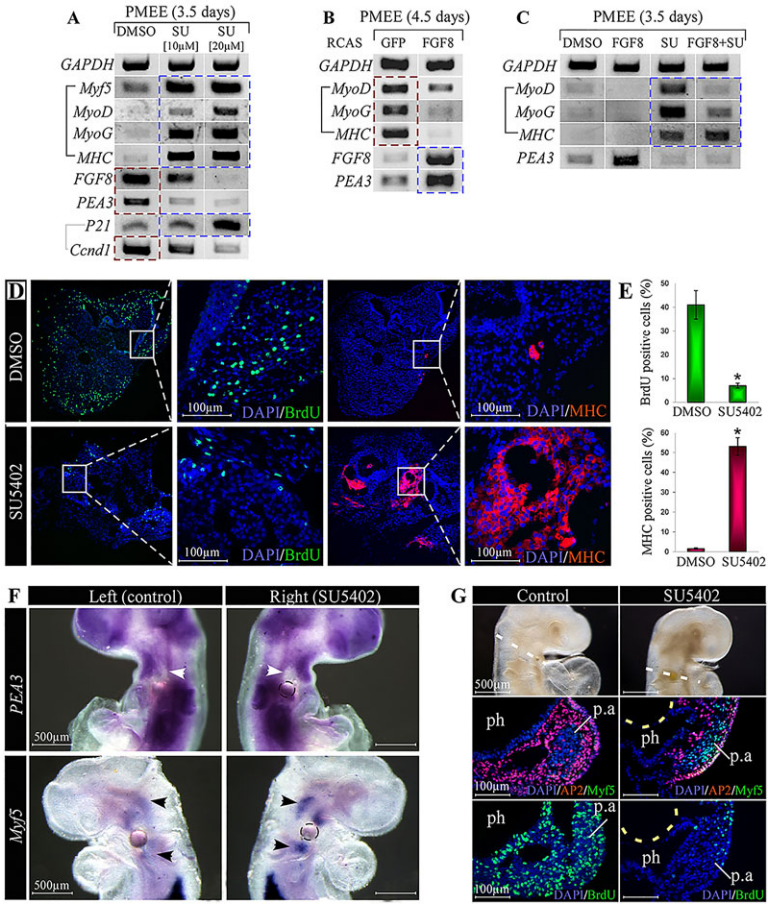

Fig. 2. Inhibition of FGF signaling promotes myogenic differentiation in the chick. (A-C) PMEE explants cultured for 3.5 or 4.5 days, treated with the FGF-signaling inhibitor SU5402 (A), infected with FGF8 RCAS viruses (B) or treated with FGF8 protein plus SU5402 (C), and subsequently analyzed by RT-PCR. The red lines indicate downregulated genes, whereas blue lines indicate genes upregulated during myogenesis. Black brackets indicate myogenic differentiation markers. These RT-PCR results represent at least three independent experiments, each composed of a pool of five explants. (D) Immunofluorescence on transverse sections of control and SU5402-treated PMEE explants stained for DAPI, BrdU and MHC. Magnifications of the boxed areas are shown as indicated. (E) Quantification of the indicated markers. Data are mean±s.d. (F,G) SU5402-soaked beads implanted into the right pharyngeal mesoderm of a chick embryo *in vivo* and subsequently analyzed by *in situ* hybridization (F) or immunofluorescence (G). Dashed yellow and black lines indicate the location of the bead; white arrowheads indicate downregulated genes; black arrowheads indicate upregulated genes; white dashed line marks the plane of sectioning at the level of the pharyngeal arches. ph, pharynx; p.a, pharyngeal arch.

viruses inhibited myogenesis (Fig. 2B). Furthermore, FGF-mediated inhibition of myogenesis was partially rescued in the presence of SU5402 (Fig. 2C).

We speculated that inhibition of FGF signaling should lead to cell cycle exit, which is the main trigger for myogenic differentiation. In line with this hypothesis, treatment of PMEE explants with SU5402 significantly reduced BrdU staining and induced myogenic differentiation (Fig. 2D, quantified in 2E). We then tested in the chick the effect of SU5402 soaked beads on myogenesis *in vivo* at both RNA and protein levels. SU5402 induced the expression of *Myf5* whereas *Pea3*, a known target of FGF signaling, was downregulated (Fig. 2F). Notably, SU5402 induced MYF5 protein expression (which is highly correlated with myogenic differentiation) (Rinon et al., 2007) and repressed cell proliferation *in vivo* (Fig. 2G). Taken together, our findings suggest that FGF signaling plays a key role in maintaining pharyngeal muscle progenitors in an undifferentiated state both *in vitro* and *in vivo*.

Activated FGF signal (reflected by pERK staining) is detected in both neural crest cells and within the myogenic mesoderm core (Fig. 1E). This finding may suggest that inhibition of FGF signaling promotes myogenic differentiation in a non-cell-autonomous manner. We have previously shown that ablation of the cranial neural crest population in chick embryos perturbed myogenic differentiation (Tzahor et al., 2003; Rinon et al., 2007). We further tested whether the addition of SU5402 would induce myogenic differentiation in the absence of neural crest cells. To this end, we used two different methods to ablate the cranial neural crest cells (Fig. 3). To confirm the efficiency of the cranial neural crest ablation procedure *in vivo*, HNK1 expression and neural crest markers were examined (Fig. 3A-F). Myogenesis was inhibited in the cranial neural crest-ablated embryos (Fig. 3C,F). This phenotype was rescued in the presence of SU5402, which strongly induced myogenic differentiation in PMEE explants of the neural crest-ablated embryos (Fig. 3C,F; marked with blue dashed lines). This experiment suggests that inhibition of FGF signaling is required cell-autonomously in the muscle progenitors, in line with experiments performed in muscle satellite cells (Fig. 5).

We next examined our explant system, to determine which intracellular signaling pathway, lying downstream of the FGF receptor, regulates myogenesis. We used several pharmacological inhibitors of different signaling pathways to test their ability to promote myogenesis in PMEE explants compared with SU5402 (Fig. 4A,B). Strikingly, inhibitors of the Raf/MEK/ERK signaling cascade induced myogenesis, whereas those against the PI3K/AKT or P38 MAPK pathways failed to do so (Fig. 4A,B). Interestingly, inhibition of PKC, which was shown to be activator of ERK, also induced myogenic differentiation.

Activation of ERK stimulates a diverse array of cellular responses. In addition to its known role in promoting cell cycle progression, it has been suggested that subcellular localization of ERK regulates distinct cellular responses (Marenda et al., 2006; Chuderland et al., 2008). ERK nuclear shuttling is mediated by a nuclear translocation sequence (NTS) within the kinase insert domain of ERK. Phosphorylation of this domain promotes ERK interaction with the nuclear importing protein, importin 7, which mediates the translocation of ERK into the nucleus via nuclear pores (Zehorai et al., 2010; Plotnikov et al., 2011) (supplementary material Fig. S2).

We hypothesized that nuclear localization of pERK promotes myogenic cell proliferation and the cytoplasmatic localization of pERK is associated with myogenic differentiation. To test this hypothesis, we blocked ERK translocation to the nucleus using a

Development (2014) 141, 2611-2620 doi:10.1242/dev.107078

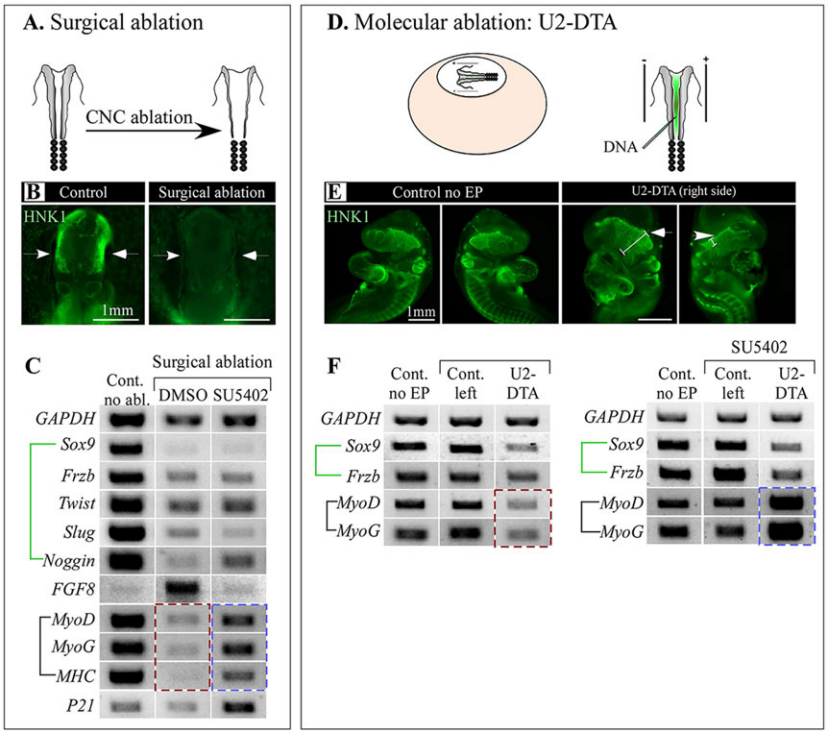

Fig. 3. SU5402 treatment can induce myogenesis following cranial neural crest ablation. (A,D) Cranial neural crest ablation using either surgical (A) or molecular (D) techniques in chick embryos. (B,E) Whole-mount immunofluorescence of control and ablated embryos stained for the neural crest marker HNK1. (C,F) PMEE explants from control or ablated chick embryos were treated with DMSO or SU5402 and further subjected for RT-PCR analysis. The red lines indicate downregulated genes that result from the neural crest ablation, whereas blue lines indicate genes upregulated as a result of the SU5402 treatment. Black brackets indicate myogenic differentiation markers; green brackets mark neural crest markers. The RT-PCR results represent three independent experiments, each composed of a pool of five explants.

competitive 18-mer myristylated peptide, termed EPE (supplementary material Fig. S2). This peptide was produced by replacing the serine residues of the SPS sequence in the kinase insertion domain (KID) of ERK2 to glutamic acid, to form phospho-mimetic EPE (Chuderland et al., 2008) (supplementary material Fig. S2). Indeed, PMEE explants treated with the EPE peptide underwent robust myogenesis (Fig. 4A). Thus, inhibition of the ERK signaling cascade or ERK nuclear translocation strongly promoted myogenic differentiation in head muscle progenitors.

We then examined the subcellular localization of ERK by immunostaining of PMEE explants. Nuclear staining of pERK along with BrdU/pHis3 staining was detected in day 1 explants, similar to its expression *in vivo* at stage 14 (Fig. 1E and Fig. 4C). In contrast, day 4 explants displayed high levels of MHC, reduced BrdU and diffuse pERK staining throughout the cytoplasm (Fig. 4D, quantified in 4F,G). Further examination of a high-resolution image of PMEE explants revealed a clear cytoplasmic expression of pERK in differentiating myoblasts (MHC^{+}), whereas nuclear pERK expressing cells did not express MHC (Fig. 4E; supplementary material Movie 1 shows the 3D reconstruction of these images). Combined, these results suggest that nuclear-to-cytoplasm translocation of ERK promotes myogenic differentiation in PMEE explants.

We then tested the effect of the EPE peptide *in vivo*. Injection of the EPE peptide into the right side of stage 10 chick embryos induced MYF5 and repressed ISL1 protein expression *in vivo* 2 days later (Fig. 4H). This result was consistent with our previous study (Harel et al., 2009), which showed that overexpression of ISL1 in chick embryos suppresses myogenic differentiation *in vivo*. Taken together, the EPE peptide induced myogenic differentiation in muscle progenitors both *in vitro* and *in vivo*.

ERK signaling is activated by numerous growth factors. In order to follow FGF-mediated ERK activation *in vivo*, we injected FGF into the right pharyngeal mesoderm of stage 10 chick embryos (Fig. 4I-K). Four hours later, FGF induced nuclear pERK expression compared with contralateral control and PBS injection (Fig. 4L-N).

In order to better resolve the effect of the EPE peptide on nuclear and cytoplasmic localization of ERK, we used mouse satellite cells derived from the lower jaw digastric muscle that originated in the pharyngeal mesoderm (Harel et al., 2009). We asked whether EPE indeed blocks ERK nuclear translocation and hence triggers myogenesis in adult muscle stem cells. Whereas ERK expression was detected in nuclei of cells treated with a scrambled (control) peptide, EPE treatment induced robust myogenic differentiation with formation of myotubes accompanied by strong cytoplasmic expression of ERK (Fig. 5A, quantified in 5B). Furthermore, both the MEK inhibitor U0126, and the EPE peptide induced myogenic differentiation of head muscle satellite cells and reduced cell proliferation (Fig. 5C,D, quantified in 5E). These findings demonstrate that ERK sequestering outside the nucleus (by blocking its nuclear translocation) can activate myogenic differentiation in embryonic and adult head muscle progenitor/stem cells.

We then examined whether the nuclear-cytoplasmic shuttling of ERK during muscle differentiation is a unique phenomenon to head muscle progenitors/stem cells or whether it could also affect trunk myogenesis. Gastrocnemius-derived mouse satellite cells treated with the EPE peptide exhibited increased cytoplasmic ERK localization and a significantly higher amount of myofibers expressing MHC compared with control (Fig. 5F, quantified in 5G,H). Next, we used stage 10 chick somite explants (Fig. 5I) treated with either the MEK inhibitor (PD184352) or with the EPE peptide. Both treatments induced myogenic differentiation (Fig. 5J). Collectively, our data suggest that inhibition of the ERK nuclear translocation strongly promotes myogenic differentiation in head and trunk muscle progenitor/stem cells.

Sprouty (Spry) genes act as inhibitors of several receptor tyrosine kinases, primarily FGF receptor signaling (Kim and Bar-Sagi, 2004; Lagha et al., 2008) (Fig. 6E). Spry1 has been recently shown to be involved in adult muscle stem cell quiescence and self-renewal during homeostasis and tissue repair (Shea et al., 2010). Because *Spry1* and *Spry2* function redundantly in several tissues, we analyzed *Spry1*$^{-/-}$;

Development (2014) 141, 2611-2620 doi:10.1242/dev.107078

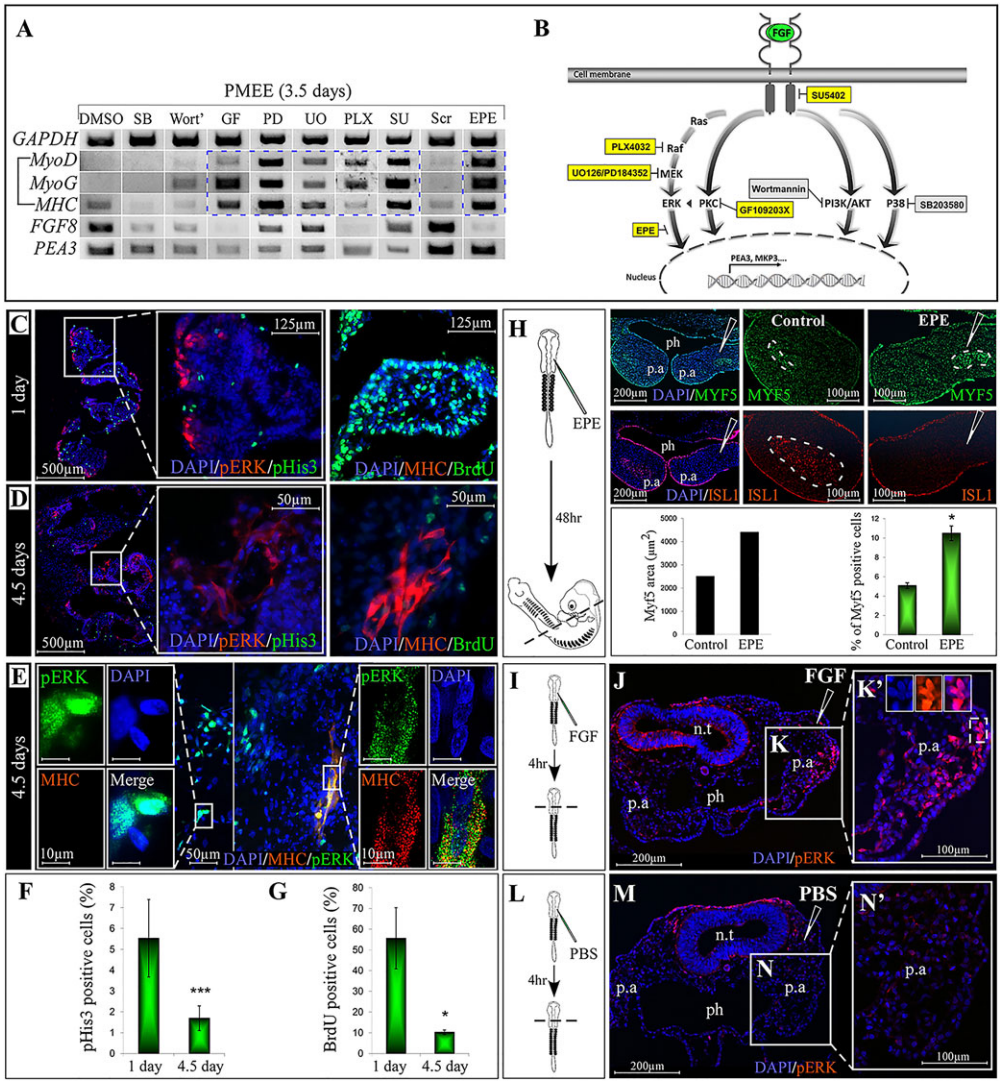

Fig. 4. Inhibition of the Raf/MEK/ERK signaling cascade or ERK nuclear translocation is sufficient to promote myogenic differentiation of head muscle progenitors in the chick. (A) RT-PCR analysis of PMEE explants treated with different pharmacological inhibitors within the FGF signaling pathways. The RT-PCR results represent at least three independent experiments, each composed of a pool of five explants. (B) A model of the various FGF signaling cascades showing the cellular targets of different pharmacological inhibitors. (C-E) Immunofluorescence of transverse sections of 1- (C) and 4.5- (D,E) day PMEE explants. Magnifications of the boxed areas are shown as indicated. (F,G) Statistical analysis of the indicated markers from C,D. Data are mean±s.d. **P*<0.05, ****P*<0.001. (H) *In vivo* administration of EPE peptide is drawn schematically on the left. Stage 10 embryos injected unilaterally with EPE peptide and incubated for 48 h. Immunofluorescence of transverse sections through the first pharyngeal arch. The mesodermal core within the first pharyngeal arch is outlined. MYF5 expression is quantified in the bottom panel either by counting MYF5-positive cells or by calculating the area of MYF5-positive cells inside the myogenic core. Data are mean±s.d. **P*<0.05. (I-N) Stage 10 embryos injected unilaterally with FGF (I) or PBS control (L), and incubated for 4 h. The plane of section is marked with a broken line. Immunofluorescence on transverse sections of FGF- (J) or PBS- (M) injected embryos stained for DAPI and pERK. The magnified areas are shown in K′,N′. n.t, neural tube; ph, pharynx; p.a, pharyngeal arch.

Spry2$^{-/-}$ (double mutants) mouse embryos, which are used as a model for increased FGF-ERK signaling (Petersen et al., 2011). At E11.5, the myogenic core within the first pharyngeal arch was reduced in the double mutants compared with the control, as evidenced by the reduced numbers of MyoD- and MyoG-expressing cells (Fig. 6A, quantified in 6B,C). pERK staining was augmented in the pharyngeal arches of the double mutants (Fig. 6F,G). In addition, the Spry double mutants contained ~3-fold increase of Pax7^{+} MyoD^{+} cells compared with control mice (Fig. 6A′, quantified in 6D). Conceivably, myogenic cells in the mutant embryos are 'stuck' at a proliferative (Pax7^{+} MyoD^{+}) state, allowing fewer cells to undergo proper myogenic differentiation. Analysis of myogenesis in the trunk of *Spry1*$^{-/-}$;*Spry2*$^{-/-}$ (double mutant) embryos revealed a clear loss of *MyoD* (RNA) and MHC (protein) in the hypaxial somites (Fig. 6H,I). Taken together, our findings suggest that ERK signaling blocks the differentiation of head and trunk muscle progenitors during mouse and chick embryogenesis.

The cellular responses regulated by ERK can be linked to various intracellular signaling mechanisms that affect the magnitude and/or the duration of ERK activation, as well as its subcellular localization. We developed a mathematical model for spatial compartmentalization of the FGF-ERK signaling cascade to better understand how this pathway regulates the progressive differentiation of muscle progenitors (detailed in the supplementary methods). The compartment model is a system of ordinary differential equations. It includes phosphorylated MEK (activated by mitogenic FGF stimuli) as well as ERK in unphosphorylated and phosphorylated states (as model variables), which can exist in both the nucleus and cytoplasm (see supplementary methods for model equations). All model results are based on analysis of the model at steady-state (~24-36 h). According to this model, when FGF levels are high, phosphorylated ERK is shuttled to the nucleus, a process that should lead to proliferation of myogenic progenitors and inhibition of myogenesis (Fig. 7A,C). Any perturbation along the FGF-ERK pathway would result in low levels of phosphorylated ERK in the nucleus, which would lead to myogenic differentiation (Fig. 7B,C, colored lines). Under both stimulatory and inhibitory conditions, the model predicts a switch-like (all-or-none) cellular response that qualitatively agrees with the behavior observed experimentally during myogenesis in the embryo and in satellite cells (Fig. 7A-D). In sum, we suggest that shuttling of MEK/ERK between the cytoplasm and the nucleus provides a stable switch between two cellular responses: myogenic proliferation and differentiation (Fig. 7D).

ERK activation can generate both graded and all-or-none (on-off) cellular outputs in distinct cell types (Fig. 7D). If we consider, in our mathematical model, the simple phosphorylation-dephosphorylation of ERK in a homogeneous environment, the model can yield only

Development (2014) 141, 2611-2620 doi:10.1242/dev.107078

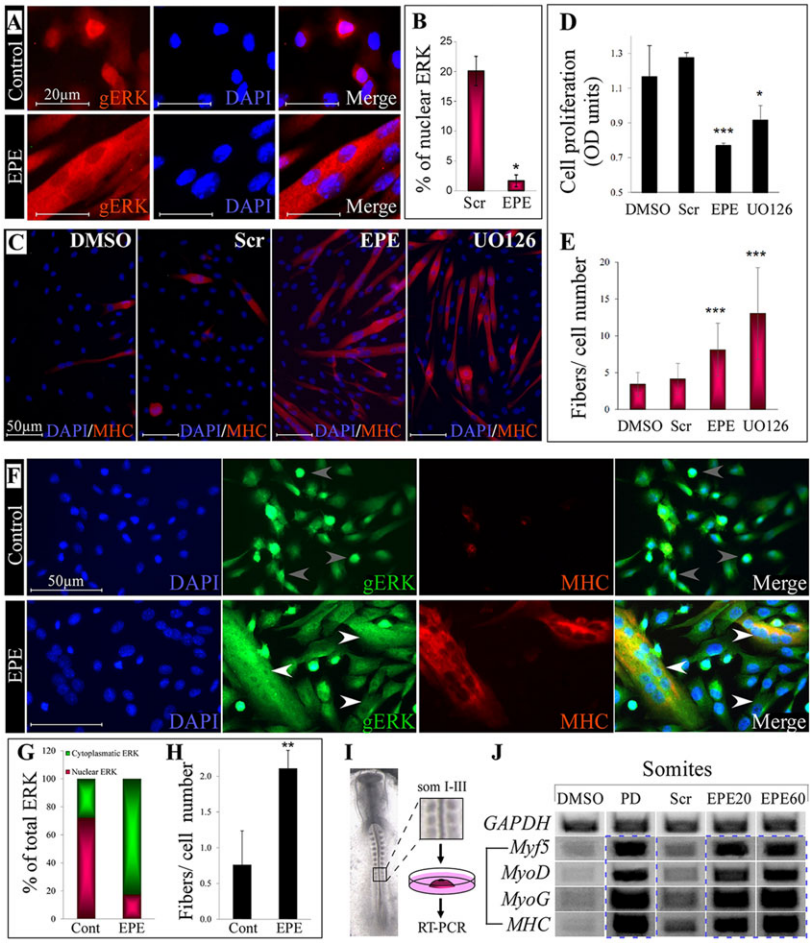

Fig. 5. Inhibition of ERK nuclear translocation promotes myogenic differentiation of head and trunk muscle satellite cells (mouse), as well as somite muscle progenitors (chick). (A-E) Analysis of head muscle mouse satellite cells. (A,C) Immunofluorescence of digastric-derived satellite cells treated with EPE or control scrambled peptides (A,C) and UO126 or DMSO control (C). (B) Quantification of the effect of EPE on ERK nuclear translocation. Data are mean ±s.d. **P*<0.05. (D) Quantification of the effects of EPE and UO126 (compared with a scrambled peptide or DMSO, respectively) after 72 h incubation on cell viability as measured by Methylene Blue assay. Data are mean±s.d. **P*<0.05, ****P*<0.001. (E) The effects of the different treatments on myogenic differentiation of head-muscle satellite cells, quantified by the amount of fibers expressing MHC per total cell number. Data are mean±s.d. ****P*<0.001. (F-H) Analysis of trunk-muscle mouse satellite cells. (F) Immunofluorescence of gastrocnemius-derived satellite cells treated with EPE or control scrambled peptides for 2 h. In order to better observe ERK translocation, cells were then stimulated with FGF8. The results indicate that EPE induces ERK cytoplasmic translocation (white arrowheads) and myogenic differentiation. (G,H) Quantification of the effect of EPE on ERK subcellular localization (G) and myogenic differentiation (H). Data are mean±s.d. ***P*<0.01. (I) Procedure used to obtain and analyze dissected somite explants from stage 10 chick embryos. (J) RT-PCR analysis of these explants treated with the indicated compounds. The RT-PCR results represent three independent experiments, each composed of a pool of five explants.

a graded response. However, by including in the model two cellular compartments and the shuttling of ERK between them, we found that this response became a bistable/ultrasensitive switch (Fig. 7D and supplementary material Fig. S3). The key feature of this spatiotemporal model is the prediction of a switch between responses, meaning that cells cannot both proliferate and differentiate simultaneously. Taken together, our findings shed light on the underlying mechanisms responsible for the cell fate switch, implicating ERK nuclear-cytoplasmic compartmentalization as a central mechanism that regulates myogenesis.

DISCUSSION

The development of skeletal muscles provides a classical paradigm with which to understand the signals and molecular events that control the proliferation and differentiation of muscle progenitors. In addition to providing basic insights into developmental biology, this area of research can be relevant to regenerative medicine, as myogenesis in adult muscle stem cells recapitulates that of the embryo (Wagers and Conboy, 2005; Bryson-Richardson and Currie, 2008).

A major challenge in the signal-transduction field is to understand how a single signaling molecule can give rise to different cellular responses, such as proliferation and differentiation. Initial insights obtained from PC12 cells revealed that transient ERK activation by epidermal growth factor (EGF) leads to proliferation whereas sustained ERK activation by nerve growth factor (NGF) leads to differentiation, showing that the duration of ERK signaling is crucial for cell-fate decisions (Marshall, 1995).

In the current study, we found a mechanism that allows the ERK signaling cascade to play a crucial role in the switch from proliferation to differentiation of muscle progenitors. We demonstrated that ERK shuttling between the nucleus (proliferation) and cytoplasm (differentiation) is the molecular mechanism underlying this switch (Fig. 8). We show that inhibition of ERK nuclear translocation is sufficient to induce myogenic progenitor/stem cell differentiation.

The relationship between proliferation and differentiation is a classic example of a biological yin and yang. In the embryo, cessation of cell proliferation is considered to be a trigger for differentiation. In most cells, proliferation is dependent on ERK signaling, which facilitates the transition through the early G1 phase of the cell cycle. We propose that proliferation-promoting signals act as suppressors of muscle differentiation during embryogenesis. Inhibition of ERK nuclear translocation promotes robust myogenic differentiation in both head and trunk muscle progenitors (Fig. 8). Thus, it seems that ERK shuttling as a key mechanism that regulates myogenesis is conserved in both embryonic and adult, as well as head and trunk muscle progenitors.

We have previously demonstrated in chick embryos that inhibitors of both Wnt and BMP signaling promote head myogenesis (Tzahor et al., 2003; Tirosh-Finkel et al., 2010). We now show that inhibition of FGF signaling in pharyngeal mesoderm progenitors promotes robust myogenic differentiation in head muscle progenitors. Both Wnt (Tzahor, 2007) and FGF signaling pathways appear to be important in maintaining the progenitor cell state in pharyngeal mesoderm and in delaying myogenic differentiation (this study; Tirosh-Finkel et al., 2010). In addition, a positive crosstalk between FGF and Wnt

Development (2014) 141, 2611-2620 doi:10.1242/dev.107078

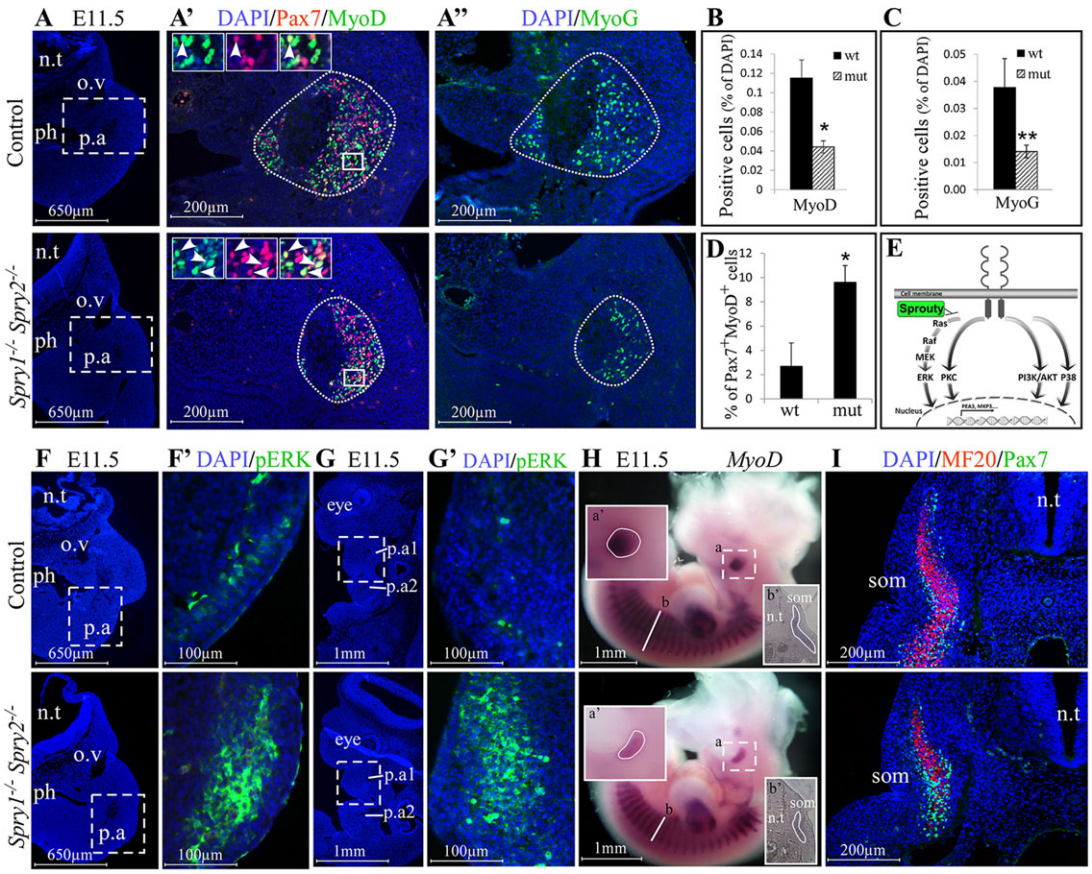

Fig. 6. Increased ERK signaling suppresses head and trunk myogenesis in the mouse. (A-A′′) Immunofluorescence on transverse sections of E11.5 control and *Spry1*$^{-/-}$;*Spry2*$^{-/-}$ double mutant embryos, at the level of the first pharyngeal arch, stained for DAPI, MyoD, Pax7 and MyoG. Dashed lines in A represent the magnified areas in A′ and A′′; dotted circular lines mark the myogenic core. Insets in A′ are higher magnifications of the boxed areas in A′. White arrowheads indicate Pax7^{+}MyoD^{+} double-positive cells. (B-D) Quantification of the indicated markers. Data are mean±s.d. **P*<0.05, ***P*<0.01. (E) Schematic representation of Sprouty-mediated inhibition of the ERK cascade. (F-G′) Similar sections to those in A (F,F′) or sagittal sections (G,G′) stained for DAPI and pERK. (H) Whole-mount *in situ* hybridization for *MyoD* on E11.5 control and *Spry1*$^{-/-}$;*Spry2*$^{-/-}$ double mutant embryos. (a′) Magnification of *MyoD* expression inside the myogenic core. (b′) Transverse section at the level of the somites (as indicated in b). (I) Immunofluorescence on transverse sections at the level of the somites, stained for DAPI, MF20 and Pax7. n.t, neural tube; o.v, otic vessel; ph, pharynx; p.a, pharyngeal arch; som, somite.

pathways reinforces this response (Dailey et al., 2005). Altogether, FGF signaling affects head myogenesis by promoting progenitor cell proliferation, consistent with previous studies (von Scheven et al., 2006; Knight et al., 2008). We revealed a negative correlation between the expression of FGF ligands and myogenesis, suggesting that the temporal regulation of FGF ligand expression controls the onset of myogenesis. What regulates FGF ligand expression in the pharyngeal arches is therefore a key question. Our previous study (Tirosh-Finkel et al., 2010) demonstrated that BMP signaling suppresses the expression of many FGF ligands, although the mechanism by which this inhibition occurs is still unclear. However, BMP signaling needs to be downregulated in order to promote skeletal myogenesis, as BMPs are potent inhibitors of both head and trunk myogenesis (Tzahor et al., 2003; Tirosh-Finkel et al., 2006). Hence, it is not trivial to assume that BMP signaling by itself shuts off FGF ligand expression, as it would block myogenesis. Thus, other regulators of FGF ligands expression are yet to be found.

In addition to contributing to the formation of skeletal elements and connective tissue in the head, cranial neural crest cells are involved in the patterning and differentiation of the head musculature (reviewed by Tzahor and Evans, 2011). Although it is generally accepted that the cranial neural crest cells influences cranial muscle formation, exactly how cranial neural crest cells participate in this process has yet to be elucidated. Neural crest ablation in the chick results in increased FGF signaling and elevated proliferation in the pharyngeal mesoderm (Fig. 3) (Waldo et al., 2005; Hutson et al., 2006; Rinon et al., 2007). These findings suggest that neural crest cells buffer proliferative signals (presumably FGFs) secreted from the endoderm and ectoderm, to promote migration and differentiation of pharyngeal mesoderm progenitors (this work; Tirosh-Finkel et al., 2010).

Sprouty proteins are known as general inhibitors of RTKs with pleiotropic roles within development. Here, we have used *Spry1*$^{-/-}$;*Spry2*$^{-/-}$ double mutant embryos as a model for increased FGF-ERK signaling (Petersen et al., 2011). However, we cannot exclude the possibility that other RTKs can also stimulate ERK signaling in these mutant mice. In addition, SU5402 inhibits FGFR signaling but can also affect other RTKs such as VEGFR and PDGFR. Which signaling pathway is therefore operated *in vivo*? Collectively, our data strongly suggest that the FGF-ERK signaling is the major signaling pathway that represses head myogenesis.

There are several unanswered questions that remain to be addressed. For example, does cytoplasmic ERK promote myogenic differentiation (or inhibits cell proliferation), and more specifically how does nuclear ERK suppress the differentiation of muscle progenitors? A plausible scenario for the effect of ERK on cell cycle progression, supported by the known functions of ERK in myogenesis (Knight and Kothary, 2011) and partially by our data (Figs 1, 2), is the following: activation of ERK and its translocation to the nucleus lead to the shuttling of p21 to

Development (2014) 141, 2611-2620 doi:10.1242/dev.107078

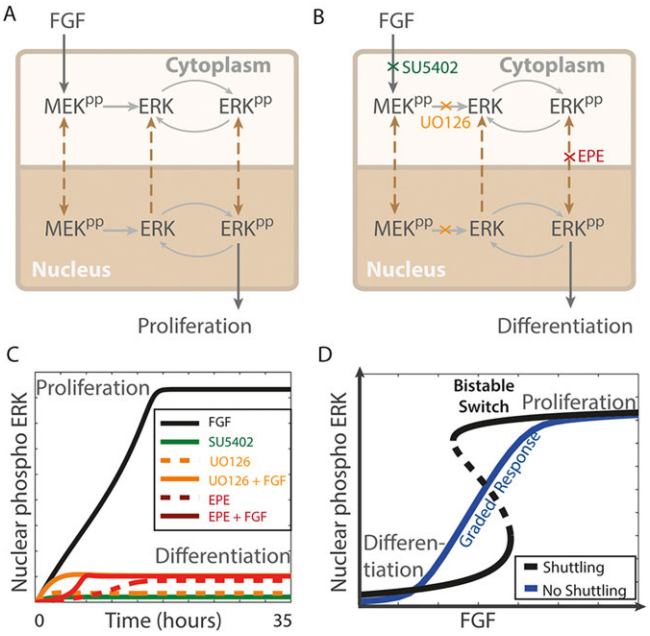

Fig. 7. Mathematical model describing the switch-like behavior of myogenic cells from proliferation to differentiation and its regulation by nuclear translocation of ERK. (A) Mechanistic model describing FGF-ERK signaling pathway. FGF signaling leads to phosphorylation of MEK and ERK in a sequential manner, followed by their translocation to the nucleus to activate target genes associated with proliferation of myogenic progenitors. (B) Inhibition of the FGF-ERK pathway leads to shuttling of ERK to the cytoplasm and consequently to myogenic differentiation. Inhibitors are SU5402 (green X), which blocks FGFR activity; UO126 (orange X), which prevents phosphorylation of ERK by MEK; EPE peptide (red X) reduces ERK translocation into the nucleus. (C) Simulated time course of the FGF-ERK pathway shows a switch taking place between FGF-treated cells in which myogenesis is inhibited and robust myogenesis in the presence of all other conditions. Low FGF signaling/SU5402, green solid line; UO126, orange dotted line; UO126+FGF, orange solid line; EPE, red dotted line; EPE+FGF, red solid line. (D) Modeling dose-response curves of phosphorylated ERK as a function of FGF levels. Shuttling of ERK between the cytoplasm and the nucleus transforms a graded response (no shuttling, blue) to a bi-stable on-off switch (shuttling, black) between the two cell fates: proliferation or differentiation.

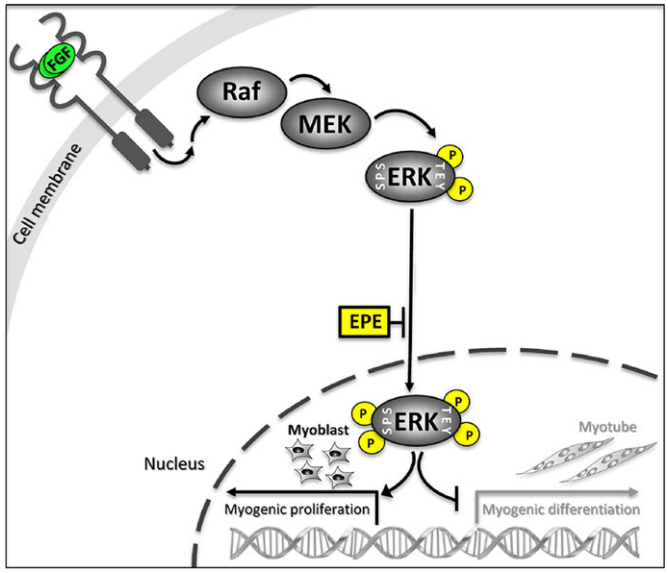

Fig. 8. ERK shuttling between the nucleus and cytoplasm regulates myogenesis. This model demonstrates that FGF-ERK signaling cascade acts to block the premature differentiation of myogenesis in the embryo. This pathway leads to the phosphorylation of ERK by MEK and its translocation to the nucleus where it promotes cell cycle progression (and can inhibit muscle differentiation). Inhibition of ERK nuclear translocation leads to robust myogenic differentiation in muscle progenitors and in muscle satellite cells.

the cytoplasm, where it undergoes ubiquitin-dependent degradation (Hwang et al., 2009) and/or ERK-dependent activation of Ccnd1, thereby enabling cell cycle progression.

Many biological processes and cell fate decisions in particular, are binary ('on-off'). These on-off cellular responses (termed ultrasensitivity and bistability) filter out extraneous 'noise', and are quickly and robustly activated, and thus can sharply alter cell fate. A broad array of signaling strategies (e.g. positive feedback loops) have been proposed to underlie this robust ultrasensitivity response (Shah and Sarkar, 2011). Recent mathematical models (Ferrell, 1998; Bhalla, 2011; Santos et al., 2012; Harrington et al., 2013) have revealed that the subcellular spatial organization of signaling molecules is best suited for generating a diverse set of cellular states, including such bistable switches. Based on both experimental and mathematical data sets, we propose that ERK shuttling between the nucleus and the cytoplasm generates a switch from proliferation to differentiation (Fig. 8). We provide a concise mechanistic model that both predicts and confirms the myogenic states found experimentally in head muscle progenitors. We propose that ERK nuclear shuttling can change a graded response into a bistable switch (Fig. 7D) (Santos et al., 2012; Harrington et al., 2013). Taken together, our findings shed light on the underlying mechanisms responsible for the stable switch from proliferation to differentiation, implicating ERK subcellular localization as the major mechanism underlying regulation of myogenesis.

Understanding the mechanism of myogenic differentiation in the embryo can shed light on numerous diseases in which this crucial process is disrupted. Our demonstration that inhibition of the ERK signaling cascade is a key step in myogenic differentiation has several implications. Rhabdomyosarcoma is a muscle tumor that expresses high levels of ERK and thus muscle progenitors do not undergo proper myogenic differentiation. Treatment of rhabdomyosarcoma-derived cell lines with the specific MEK inhibitor U0126 reversed the transformed phenotype, and induced growth arrest and myogenic differentiation, both *in vitro* and *in vivo* (Marampon et al., 2006). In addition, ERK was found to be involved in the pathogenesis of muscle wasting (termed cachexia) in individuals with cancer (Penna et al., 2011). Taken together, we propose that ERK signaling is a key process in the control of cell cycle progression and differentiation during embryogenesis and adulthood, under normal and pathological conditions.

MATERIALS AND METHODS

Eggs, embryos and explant culture assays

Fertilized white eggs were incubated for 1-6 days at 38.5°C in a humidified incubator to reach Hamburger & Hamilton stages 8-28. PMEE explants were cultured for 1-5 days on a collagen drop covered with 700 µl of dissection medium (10% fetal calf serum, 2.5% chick embryo extract and 1% penicillin/streptomycin in αMEM medium) in a four-well plate. Pharmacological reagents that were added to the medium are listed below. Alternatively, PMEE explants were infected with replication-competent retroviruses (RCAS) expressing FGF8 (Tzahor et al., 2003). Gene expression was measured at the RNA level following RT-PCR or at the protein level following immunofluorescence on cryosections.

The following reagents were added directly to the explant dissection medium: UO126, SU5402 and SB203580 (20 µM, Calbiochem); PLX-4032 (2 µM, Selleck); PD184352 (2 µM, Sigma); GF 109203X (6 µM,

Development (2014) 141, 2611-2620 doi:10.1242/dev.107078

Calbiochem); wortmannin (100 nM, Sigma); BAPTA-AM (10 μM, Sigma); EPE peptide (Myr-GQLNHILGILGEPEQEDL-NH2) (20 μM, Peptide 2.0); and SCR peptide (Myr-GNILSQELPHSGDLQIGL-NH2) (20 μM, Peptide 2.0).

RNA analysis

Total RNA was extracted using Qiagene RNeasy micro kit (Qiagene), followed by reverse transcription using the cDNA Reverse Transcription kit (Applied Biosystems). The cDNA product was then amplified using different sets of primers via semi-quantitative RT-PCR or quantitative real time PCR (qRT-PCR) (supplementary material Table S1 and Table S2, respectively). Gene expression analysis for representative genes were validated by qRT-PCR, using the SYBER GREEN PCR Master mix and Step One Plus Real Time PCR system instrument and software (Applied Biosystems). Primer sets were designed using Primer Express3 (Applied Biosystems) or the Universal ProbeLibrary Assay Design Center (Roche Applied Science). To avoid amplification of contaminating genomic DNA, primers for qRT-PCR were designed to be located at the exon-exon junction. The comparative Ct method was used for quantification of transcripts according to the manufacturer's protocol. Measurement of ΔCt was performed in triplicate. *Gapdh* (glyceraldehyde 3-phosphate dehydrogenase) was used as the endogenous control gene.

BrdU assay for explant culture

A BrdU assay was used in order to validate cell proliferation. After 1-5 days in culture, PMEE explants were incubated for an additional 45 min with final concentration of 10 μM BrdU. To stop the reaction, the explants were fixed in 4% PFA, and BrdU incorporation was assessed by immunofluorescence staining. Cell proliferation is measured as the proportion of BrdU-positive cells of total cell nuclei.

Bead implantation and peptides injection experiments

Resin beads (Sigma) were incubated with 5 mM SU5402 or DMSO overnight at 4°C. Beads were rinsed in PBS and inserted into the right pharyngeal mesoderm of stage 10 chick embryos using tungsten needles. Alternatively, 100 μM EPE or SCR peptides were injected into the right pharyngeal mesoderm of stage 10-12 chick embryos. Embryos were returned to the incubator for an additional 24-48 h, and then fixed in 4% PFA and subjected for *in situ* hybridization or immunofluorescence analyses.

Staining procedures

Whole-mount *in situ* hybridization was performed as previously reported (Tirosh-Finkel et al., 2006). For immunofluorescence, embryos and explants were fixed with 4% PFA in PBS. For frozen sections, embryos and explants were transferred to 30% sucrose in double-distilled water overnight at 4°C, embedded in OCT and sectioned at ∼7 μm, using a Leica cryostat. Sections from explants were further fixed in pre-cold (−20°C) acetone. Paraffin sections were deparaffinized using standard methods, and subjected to sodium citrate antigen retrieval. Sections were then permeabilized for 15 min with 0.1%-0.25% Triton X-100 and blocked for 1 h with 5% horse serum, 1% bovine serum albumin and 0.1% Tween 20 in PBS. Sections were sequentially incubated with the appropriate primary antibodies diluted in blocking solution as listed below. DAPI was diluted 1:2000. Secondary antibodies used were: Cy2-, Cy3- or Cy5-conjugated anti-mouse or anti-rabbit IgG (1:100, Jackson ImmunoResearch; #111-225-003, #115-165-003 or #111-175-144); and Cy3-conjugated anti-mouse IgG1 and Cy5-conjugated anti-mouse IgG2b (1:100, Jackson ImmunoResearch; #115-165-205 or #115-175-207, respectively.). Images were obtained with a Nikon 90i florescent microscope using the ImagePro+ program (Media Cybernetics) and assembled using Photoshop CS software (Adobe). Quantification of the staining results was obtained using ImagePro+ software. Additional images were obtained using a DeltaVision Elite system (Applied Precision) on an Olympus IX71 inverted microscope, running SoftWorX 6.0. Fluorescent images were acquired at 20× and 100× magnifications (UPlanSApo 20×/0.85 and UPlanFl 100×/1.3 objectives, Olympus) by a CoolSnap HQ2 CCD camera (Roper Scientific). 3D imaging was obtained by a series of *z*-sections taken at 0.2 μm intervals. Image deconvolution was performed using Imaris (Bitplane). The staining results were quantified using ImagePro+ software, based on ≥5 sections from at least two different embryos, and confirmed using a *t*-test: $*P<0.05$; $**P<0.01$; $***P<0.001$.

The following antibodies were used for immunofluorescence: AP2 (3B5 or 5E4) (1:20 or 1:5, respectively, DSHB); BrdU (G3G4) (1:100, DSHB); general ERK (1:400, M5670 Sigma); HNK (CD57) (1:80, BD Pharmingen); Isl1 (1:1, DSHB); MHC (MF20) (1:5, DSHB); Myf5 (1:500, a generous gift from Bruce Paterson, NIH, USA); MyoD (1:100, Santa Cruz; sc-760 or sc-32758); MyoG (F5Da) (1:20, DSHB); Pax7 (1:5, DSHB); pERK (M8159) (1:200, Sigma); pHis3 (1:400, Santa Cruz; sc-8656).

Neural crest ablation

Cranial neural crest cells were ablated from chick embryos using two different techniques. Surgical ablation was performed by physically ablating the dorsal neural tube just before the neural crest cells start to delaminate (∼stage 8) as previously described (Tzahor et al., 2003; Rinon et al., 2007). Alternatively we used a molecular ablation technique that was established by the Marcelle lab (Rios et al., 2011) to ablate neural crest cells by electroporation of a DTA construct under the control of a neural-crest-specific promoter (U2-DTA: the U2 is an evolutionary conserved *Sox10* enhancer sequence, cloned upstream to the diphtheria toxin gene).

Satellite cell culture

Isolation of satellite cells was performed as previously described (Harel et al., 2009). Briefly, wild-type female mice 3-4 weeks old (ICR strain) were sacrificed, and the digastric or gastrocnemius muscles were dissected and minced, followed by enzymatic dissociation at 37°C with 0.25% trypsin-EDTA for 30 min. Cells were collected, and trypsinization of the remaining undigested tissue was repeated twice. After 70 mm filtration (Cell Tricks), cells were cultured in proliferation medium (BIO-AMF-2, Biological Industries). For ERK inhibition, digastric-muscle satellite cells were grown for 2-3 days in starvation medium (DMEM with 50% BIO-AMF-2) supplemented with U0126 (10 μM, Calbiochem), DMSO, EPE or SCR peptide (10-20 μM, Peptide 2.0). Alternatively, gastronome-derived satellite cells were cultured overnight in proliferation medium, then the medium was replaced to starvation medium for 4 h and treated with EPE for an additional 2 h prior to 15 min of FGF8 stimuli (250 ng/ml). The myogenic differentiation process was quantified by the amount of fibers expressing MHC (MF20) per total cell number (DAPI). The number of viable cells was measured by Methylene Blue assay after 72 h incubation with the indicated treatments.

Sprouty mutant mice

Embryos deficient for *Spry1* and *Spry2* were produced as previously reported (Petersen et al., 2011). Embryos were fixed and embedded in paraffin. Paraffin sections were subjected for immunofluorescence analysis.

Acknowledgements

We deeply thank Liat Buzaglo, Prof. Menahem Segal (WIS), Calanit Raanan, the Department of Veterinary Resources (WIS), Prof. Christophe Marcelle, Dr Olivier Serralbo (ARMI, Australia) and Bruce Paterson (NIH) for technical help and reagents.

Competing interests

The authors declare no competing financial interests.

Author contributions

I.M. and E.T. developed the concepts and approach, analyzed the data for these studies and wrote the manuscript, with the remaining authors commenting on the manuscript. I.M. performed most of the experiments with help from H.H.A., Y.Y.R., A.P. and S.C. The mathematical model was developed and written by H.A.H. and M.P.H.S.

Funding

This work was supported by grants to E.T. from the European Research Council, Israel Science Foundation, United States-Israel Binational Science Foundation, German Israeli Foundation and Association Française Contre les Myopathies. M.P.H.S. and H.A.H. gratefully acknowledge support from a Leverhulme Trust Grant. O.D.K. is supported by the National Institutes of Health [R01-DE021420]. Deposited in PMC for release after 12 months.

Supplementary material

Supplementary material available online at
http://dev.biologists.org/lookup/suppl/doi:10.1242/dev.107078/-/DC1

References

Bhalla, U. S. (2011). Trafficking motifs as the basis for two-compartment signaling systems to form multiple stable states. *Biophys. J.* **101**, 21-32.

Bryson-Richardson, R. J. and Currie, P. D. (2008). The genetics of vertebrate myogenesis. *Nat. Rev. Genet.* **9**, 632-646.

Buckingham, M. (2006). Myogenic progenitor cells and skeletal myogenesis in vertebrates. *Curr. Opin. Genet. Dev.* **16**, 525-532.

Buckingham, M. and Vincent, S. D. (2009). Distinct and dynamic myogenic populations in the vertebrate embryo. *Curr. Opin. Genet. Dev.* **19**, 444-453.

Chuderland, D., Konson, A. and Seger, R. (2008). Identification and characterization of a general nuclear translocation signal in signaling proteins. *Mol. Cell* **31**, 850-861.

Dailey, L., Ambrosetti, D., Mansukhani, A. and Basilico, C. (2005). Mechanisms underlying differential responses to FGF signaling. *Cytokine Growth Factor Rev.* **16**, 233-247.

Ferrell, J. E., Jr (1998). How regulated protein translocation can produce switch-like responses. *Trends Biochem. Sci.* **23**, 461-465.

Grifone, R. and Kelly, R. G. (2007). Heartening news for head muscle development. *Trends Genet.* **23**, 365-369.

Harel, I., Nathan, E., Tirosh-Finkel, L., Zigdon, H., Guimarães-Camboa, N., Evans, S. M. and Tzahor, E. (2009). Distinct origins and genetic programs of head muscle satellite cells. *Dev. Cell* **16**, 822-832.

Harrington, H. A., Feliu, E., Wiuf, C. and Stumpf, M. P. H. (2013). Cellular compartments cause multistability and allow cells to process more information. *Biophys. J.* **104**, 1824-1831.

Heller, H., Gredinger, E. and Bengal, E. (2001). Rac1 inhibits myogenic differentiation by preventing the complete withdrawal of myoblasts from the cell cycle. *J. Biol. Chem.* **276**, 37307-37316.

Hutson, M. R., Zhang, P., Stadt, H. A., Sato, A. K., Li, Y.-X., Burch, J., Creazzo, T. L. and Kirby, M. L. (2006). Cardiac arterial pole alignment is sensitive to FGF8 signaling in the pharynx. *Dev. Biol.* **295**, 486-497.

Hwang, C. Y., Lee, C. and Kwon, K.-S. (2009). Extracellular signal-regulated kinase 2-dependent phosphorylation induces cytoplasmic localization and degradation of p21Cip1. *Mol. Cell. Biol.* **29**, 3379-3389.

Jones, N. C., Fedorov, Y. V., Rosenthal, R. S. and Olwin, B. B. (2001). ERK1/2 is required for myoblast proliferation but is dispensable for muscle gene expression and cell fusion. *J. Cell Physiol.* **186**, 104-115.

Kim, H. J. and Bar-Sagi, D. (2004). Modulation of signalling by Sprouty: a developing story. *Nat. Rev. Mol. Cell Biol.* **5**, 441-450.

Knight, J. D. R. and Kothary, R. (2011). The myogenic kinome: protein kinases critical to mammalian skeletal myogenesis. *Skelet. Muscle* **1**, 29.

Knight, R. D., Mebus, K. and Roehl, H. H. (2008). Mandibular arch muscle identity is regulated by a conserved molecular process during vertebrate development. *J. Exp. Zoolog. B Mol. Dev. Evol.* **310B**, 355-369.

Lagha, M., Kormish, J. D., Rocancourt, D., Manceau, M., Epstein, J. A., Zaret, K. S., Relaix, F. and Buckingham, M. E. (2008). Pax3 regulation of FGF signaling affects the progression of embryonic progenitor cells into the myogenic program. *Genes Dev.* **22**, 1828-1837.

Li, J. and Johnson, S. E. (2006). ERK2 is required for efficient terminal differentiation of skeletal myoblasts. *Biochem. Biophys. Res. Commun.* **345**, 1425-1433.

Marampon, F., Ciccarelli, C. and Zani, B. M. (2006). Down-regulation of c-Myc following MEK/ERK inhibition halts the expression of malignant phenotype in rhabdomyosarcoma and in non muscle-derived human tumors. *Mol. Cancer* **5**, 31.

Marcelle, C., Wolf, J. and Bronner-Fraser, M. (1995). The in vivo expression of the FGF receptor FREK mRNA in avian myoblasts suggests a role in muscle growth and differentiation. *Dev. Biol.* **172**, 100-114.

Marenda, D. R., Vrailas, A. D., Rodrigues, A. B., Cook, S., Powers, M. A., Lorenzen, J. A., Perkins, L. A. and Moses, K. (2006). MAP kinase subcellular localization controls both pattern and proliferation in the developing Drosophila wing. *Development* **133**, 43-51.

Marics, I., Padilla, F., Guillemot, J. F., Scaal, M. and Marcelle, C. (2002). FGFR4 signaling is a necessary step in limb muscle differentiation. *Development* **129**, 4559-4569.

Marshall, C. J. (1995). Specificity of receptor tyrosine kinase signaling: transient versus sustained extracellular signal-regulated kinase activation. *Cell* **80**, 179-185.

Noden, D. M. (1983). The role of the neural crest in patterning of avian cranial skeletal, connective, and muscle tissues. *Dev. Biol.* **96**, 144-165.

Noden, D. M. and Francis-West, P. (2006). The differentiation and morphogenesis of craniofacial muscles. *Dev. Dyn.* **235**, 1194-1218.

Olwin, B. B. and Rapraeger, A. (1992). Repression of myogenic differentiation by aFGF, bFGF, and K-FGF is dependent on cellular heparan sulfate. *J. Cell Biol.* **118**, 631-639.

Penna, F., Busquets, S., Pin, F., Toledo, M., Baccino, F. M., López-Soriano, F. J., Costelli, P. and Argilés, J. M. (2011). Combined approach to counteract experimental cancer cachexia: eicosapentaenoic acid and training exercise. *J. Cachexia Sarcopenia Muscle* **2**, 95-104.

Petersen, C. I., Jheon, A. H., Mostowfi, P., Charles, C., Ching, S., Thirumangalathu, S., Barlow, L. A. and Klein, O. D. (2011). FGF signaling regulates the number of posterior taste papillae by controlling progenitor field size. *PLoS Genet.* **7**, e1002098.

Plotnikov, A., Chuderland, D., Karamansha, Y., Livnah, O. and Seger, R. (2011). Nuclear extracellular signal-regulated kinase 1 and 2 translocation is mediated by casein kinase 2 and accelerated by autophosphorylation. *Mol. Cell. Biol.* **31**, 3515-3530.

Rinon, A., Lazar, S., Marshall, H., Buchmann-Moller, S., Neufeld, A., Elhanany-Tamir, H., Taketo, M. M., Sommer, L., Krumlauf, R. and Tzahor, E. (2007). Cranial neural crest cells regulate head muscle patterning and differentiation during vertebrate embryogenesis. *Development* **134**, 3065-3075.

Rios, A. C., Serralbo, O., Salgado, D. and Marcelle, C. (2011). Neural crest regulates myogenesis through the transient activation of NOTCH. *Nature* **473**, 532-535.

Sambasivan, R., Kuratani, S. and Tajbakhsh, S. (2011). An eye on the head: the development and evolution of craniofacial muscles. *Development* **138**, 2401-2415.

Santos, S. D. M., Wollman, R., Meyer, T. and Ferrell, J. E., Jr. (2012). Spatial positive feedback at the onset of mitosis. *Cell* **149**, 1500-1513.

Shah, N. A. and Sarkar, C. A. (2011). Robust network topologies for generating switch-like cellular responses. *PLoS Comput. Biol.* **7**, e1002085.

Shea, K. L., Xiang, W., LaPorta, V. S., Licht, J. D., Keller, C., Basson, M. A. and Brack, A. S. (2010). Sprouty1 regulates reversible quiescence of a self-renewing adult muscle stem cell pool during regeneration. *Cell Stem Cell* **6**, 117-129.

Tirosh-Finkel, L., Elhanany, H., Rinon, A. and Tzahor, E. (2006). Mesoderm progenitor cells of common origin contribute to the head musculature and the cardiac outflow tract. *Development* **133**, 1943-1953.

Tirosh-Finkel, L., Zeisel, A., Brodt-Ivenshitz, M., Shamai, A., Yao, Z., Seger, R., Domany, E. and Tzahor, E. (2010). BMP-mediated inhibition of FGF signaling promotes cardiomyocyte differentiation of anterior heart field progenitors. *Development* **137**, 2989-3000.

Trainor, P. A., Tan, S. S. and Tam, P. P. (1994). Cranial paraxial mesoderm: regionalisation of cell fate and impact on craniofacial development in mouse embryos. *Development* **120**, 2397-2408.

Tzahor, E. (2007). Wnt/beta-catenin signaling and cardiogenesis: timing does matter. *Dev. Cell* **13**, 10-13.

Tzahor, E. and Evans, S. M. (2011). Pharyngeal mesoderm development during embryogenesis: implications for both heart and head myogenesis. *Cardiovasc. Res.* **91**, 196-202.

Tzahor, E., Kempf, H., Mootoosamy, R. C., Poon, A. C., Abzhanov, A., Tabin, C. J., Dietrich, S. and Lassar, A. B. (2003). Antagonists of Wnt and BMP signaling promote the formation of vertebrate head muscle. *Genes Dev.* **17**, 3087-3099.

von Scheven, G., Alvares, L. E., Mootoosamy, R. C. and Dietrich, S. (2006). Neural tube derived signals and Fgf8 act antagonistically to specify eye versus mandibular arch muscles. *Development* **133**, 2731-2745.

Wagers, A. J. and Conboy, I. M. (2005). Cellular and molecular signatures of muscle regeneration: current concepts and controversies in adult myogenesis. *Cell* **122**, 659-667.

Waldo, K. L., Hutson, M. R., Stadt, H. A., Zdanowicz, M., Zdanowicz, J. and Kirby, M. L. (2005). Cardiac neural crest is necessary for normal addition of the myocardium to the arterial pole from the secondary heart field. *Dev. Biol.* **281**, 66-77.

Zehorai, E., Yao, Z., Plotnikov, A. and Seger, R. (2010). The subcellular localization of MEK and ERK–a novel nuclear translocation signal (NTS) paves a way to the nucleus. *Mol. Cell. Endocrinol.* **314**, 213-220.